Heliyon 10 (2024) e30102

Contents lists available at ScienceDirect

Heliyon

journal homepage: www.cell.com/heliyon

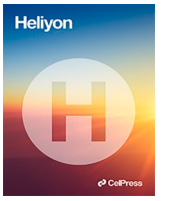

Research article

Synthesis and anti-inflammatory activity of benzimidazole derivatives; an in vitro, in vivo and in silico approach

Shaher Bano, Humaira Nadeem *, Iqra Zulfiqar, Tamseela Shahzadi, Tayyaba Anwar, Asma Bukhari, Syed Muzzammil Masaud

Department of Pharmaceutical Chemistry, Riphah Institute of Pharmaceutical Sciences, Riphah International University, Islamabad, Pakistan

ARTICLE INFO

Keywords:
Benzimidazole derivatives
Anti-inflammatory activity
Computational studies
COX
Aldose reductase
Phospholipase A2

ABSTRACT

Many non-steroidal anti-inflammatory drugs (NSAIDs) concurrently inhibit both COX-1 and COX-2, with a preference for specifically targeting COX-2 due to its significant involvement in various pathologies. In addition to COX enzymes, several other targets, including Aldose reductase, Aldo-ketoreductase family 1-member C2, and Phospholipase A2, have been identified as contributors to inflammation and a myriad of other diseases.

In this context, a series of 2-substituted benzimidazole derivatives was synthesized and assessed for their anti-inflammatory potential through both in vitro and in vivo assays. Molecular docking studies were conducted to elucidate the mechanism of action of these compounds against COX enzymes and other therapeutic targets associated with NSAIDs, such as Aldose reductase, AIKRC, and Phospholipase A2.

Among the synthesized compounds, B2, B4, B7, and B8 demonstrated IC50 values lower than the standard ibuprofen, as determined by the Luminol-enhanced chemiluminescence assay. Validation of these findings was achieved through an in vivo carrageenan-induced mice paw edema model, confirming a comparable anti-inflammatory effect to diclofenac sodium observed in vitro. Notably, these compounds exhibited significant binding affinity with all therapeutic targets investigated in this study.

These results suggest that the newly synthesized derivatives possess noteworthy anti-inflammatory potential, warranting further exploration for the development of novel multi-targeting inhibitors.

1. Introduction

The pervasive impact of inflammation and pain on healthcare has prompted an urgent need for effective management strategies. Addressing inflammation and pain involves a systematic approach, wherein classical non-steroidal anti-inflammatory drugs (NSAIDs), selective cyclooxygenase (COX) inhibitors, corticosteroids, and immunosuppressive agents are administered. Among these, NSAIDs stand out as highly effective drug choices. Nonetheless, corticosteroids are frequently prescribed in conjunction to achieve a synergistic reduction in inflammation. Both classes of agents exert their therapeutic effects through the inhibition of the biosynthesis of

* Corresponding author.
E-mail addresses: sshaherbano5@gmail.com (S. Bano), muzzammil.masaud@riphah.edu.pk, humaira.nadeem@riphah.edu.pk (H. Nadeem), iqra28841@gmail.com (T. Shahzadi), t.t.shahzadi@gmail.com (T. Anwar), bukhariasma31@gmail.com (A. Bukhari), tayyaba.anwar@riphah.edu.pk (S.M. Masaud).

https://doi.org/10.1016/j.heliyon.2024.e30102
Received 30 November 2023; Received in revised form 18 April 2024; Accepted 19 April 2024
Available online 26 April 2024

prostaglandins and thromboxane derived from arachidonic acid.

NSAIDs have been implicated in mucosal injury, contributing to chronic gastritis, specifically chemical or reactive gastritis. The gastrointestinal side effects of NSAIDs selectively impact the gastro-duodenal mucosa through the inhibition of COX-1 [1]. There is a critical need for target-specific potent anti-inflammatory agents to mitigate COX-associated inflammatory diseases. In addition to COX, other pivotal targets, including Phospholipase A2 (PLA2) [2], Aldose Reductase (AR) [3], and Aldo-ketoreductase family 1 member C2 (ARK1C2), are of significant importance in the screening of anti-inflammatory compounds.

Concurrently targeting multiple opioid receptors represents a potential avenue for pain management. Multitarget-capable ligands have indeed yielded an augmented pharmacological profile. The emergence of polypharmacology as a novel therapeutic approach involves designing or applying pharmacological drugs that act on multiple molecular targets or engage various biochemical pathways. This approach opens up a new research direction for treating challenging diseases. Employing a polypharmacological strategy, one method to develop novel analgesics with heightened efficacy and reduced side effects involves creating a singular medication with the capability to modulate several biochemical pathways involved in pain control.

Phospholipases A2 (PLA2s) play a pivotal role in diverse inflammatory responses by hydrolyzing glycerol to release arachidonic acid and lysophosphatidic acid. Subsequently, cyclooxygenases modify arachidonic acid into active compounds known as eicosanoids, including leukotrienes and prostaglandins, categorized as inflammatory mediators. Experimental evidence suggests that PLA2 can induce the release of histamine in human basophils [4]. Additionally, PLA2 exhibits modulatory effects on various aspects of the inflammatory response to microorganisms and participates in the degradation of phospholipid membranes of Gram-negative bacteria [5]. Clearly, PLA2 performs diverse biological roles in host defense, the generation of lipid mediators, and the amplification of inflammatory reactions.

The enzyme Aldose reductase (AR) is generally involved in glucose metabolism by catalyzing the polyol pathway. Recent studies implicate AR's catalytic activity in regulating several inflammatory diseases, such as asthma, sepsis, and atherosclerosis. Notably, several AR inhibitors are in different phases of FDA approval for diabetic complications, underscoring the safety of targeting AR for inflammation treatment [6].

Aldo-keto reductase family 1, member B1 (AKR1B1), a reduced form of the nicotinamide-adenine dinucleotide phosphate (NADPH)-dependent enzyme, catalyzes the reduction of various ketones and aldehydes to the corresponding alcohol. It exhibits high expression levels in several organs, including the brain, kidneys, heart, retina, lungs, and liver. AKR1B1 expression levels correlate with oxidative stress, such as vascular inflammation and alcoholic liver disease. AKR1B1 regulates inflammatory responses in asthma via NF-Kappa-B mediated downstream signaling, and its inhibition can decrease airway suppression [7]. Experimental evidence further suggests that AKR1B1 is involved in various pathological processes, including inflammation [8–10], cancer such as epithelial-mesenchymal transition (EMT) [11], and angiogenesis [12,13].

Therefore, it is imperative that drugs developed against COX enzymes undergo screening against other anti-inflammatory therapeutic targets. This approach may lead to the identification of new lead compounds for inhibiting key players in inflammation. Considering these observations, it is highly important to investigate anti-inflammatory agents as lead molecules concurrently with the screening of recently discovered drug targets.

The benzimidazole nucleus, referred to as the 'Master Key' owing to its presence in numerous medicinal compounds, exhibits a versatile role. Substituting benzimidazole at various positions holds the potential to significantly enhance the overall physicochemical, metabolic, and pharmacokinetic properties of synthesized compounds. Several compounds containing the benzimidazole moiety have received approval from the Food and Drug Administration (FDA) as proton pump inhibitors and antifungal drugs, exemplified by omeprazole and albendazole. Benzimidazole has demonstrated diverse activities, including anti-fungal [14], anthelmintic, anti-asthmatic, anti-diabetic [15], antihypertensive [16], anti-parasitic [17], anti-histaminic [18], gastro-protective [19], antibacterial [20], anticoagulant [21], anti-obesity, antioxidant [22], antitumor, and anti-inflammatory [23] effects.

Benzimidazole belongs to a category of heterocyclic aromatic organic compounds characterized by a core structural feature. This feature entails a six-membered benzene ring fused to the 4 and 5 positions of a five-membered imidazole ring system. The hydrogen atom bonded to nitrogen in the 1 position of the benzimidazole nucleus undergoes tautomerization easily, leading to isomerization in resulting compounds. Moreover, the NH group within benzimidazole displays both relatively strong acidic and weakly basic properties [24,25].

Five novel pincer-type Ni(II)-Schiff-base complexes have been successfully synthesized and thoroughly characterized using diverse spectroscopic methods. Additionally, the structural authenticity of these complexes was verified through single-crystal X-ray analysis. Furthermore, the catalytic efficacy of the Ni(II) complexes has been showcased in facilitating the synthesis of a range of 2-substituted benzimidazoles from different aldehydes and *o*-phenylenediamine substrates [26].

The structure of 1-(Thiophen-2-ylmethyl)-2-(thiophen2-yl)-1H-benzimidazole reveals that the benzimidazole ring exhibits a nearly planar conformation. Furthermore, the crystal lattice stabilization is achieved through intermolecular C–H···N and C–H··· π interactions [27].

Furthermore, in pursuit of synthesizing a bifunctional metal–organic complex (MOC) with enhanced adsorption capabilities for environmental remediation, a novel approach was undertaken. This involved the synthesis of a functional MOC designed to exhibit improved adsorption capacity and exceptional ability to separate organic hazardous dyes from wastewater. In this endeavor, researchers explored the utilization of an asymmetrical rigid nitrogen donor (N-donor) ligand, specifically 2-(2-aminophenylbenzimidazole) (L1), in the development of a new Zn(II)-based metal–organic complex denoted as [Zn(L1)(Cl)2] [28].

Numerous studies have comprehensively examined the diverse pharmacological activities associated with benzimidazole and its derivatives. This paper focuses specifically on the role of benzimidazole derivatives as analgesic and anti-inflammatory agents, elucidating their impact on a range of therapeutic targets. These targets include the cyclooxygenase (COX) enzyme, transient receptor

potential vanilloid-1 (TRPV-1) ion channels, cannabinoid receptors, bradykinin receptors, specific cytokines, and 5-lipoxygenase activating protein (FLAP) [29].

Benzimidazole derivative metal complexes exhibit promising antimicrobial efficacy against a spectrum of pathogens including *Escherichia coli*, *Pseudomonas aeruginosa*, and *Staphylococcus aureus* [30].

The distinctive structural attributes of benzimidazole, coupled with the diverse biological activities exhibited by its derivatives, position it as a privileged structure in the realm of drug discovery. Notably, the benzimidazole scaffold has recently garnered recognition as a preferred pharmacophore for crafting analgesic and anti-inflammatory agents that exert activity on various clinically approved targets [31].

Zinc(II) phthalocyanine derivatives with peripherally tetra-benzimidazole unit's substitution have been reported to possess favorable photophysical and photochemical characteristics [32].

The present study was designed to synthesize novel aminomethyl derivatives of benzimidazole and investigate there in vitro and in vivo anti-inflammatory effects. Additionally, these synthesized derivatives were subjected to analysis for their affinities with four distinct therapeutic targets associated with the inflammatory pathway, utilizing in silico approaches.

2. Materials and methods

2.1. Experimental

The purification of all synthesized compounds was accomplished through recrystallization using an appropriate solvent. The purity of the compounds was subsequently confirmed via thin-layer chromatography on silica gel F254. Characterization of the synthesized compounds was conducted through spectrophotometric analyses, specifically Fourier-transform infrared spectroscopy (FTIR) using a Thermoscientific NICOLET IS10 Spectrophotometer, and proton nuclear magnetic resonance (1H NMR) using a Bruker AM-300 Spectrophotometer. DMSO and chloroform were employed as solvents in these analyses.

2.1.1. General procedure for the synthesis of benzimidazole derivatives

A solution of benzene-1,2-diamine (0.1 mol) and 2-chloroacetic acid (0.1 mol) underwent reflux for 3 h in 4 N hydrochloric acid (50 ml) on a water bath at 100°C. Following reflux, the reaction mixture was cooled and then alkalized with ammonium hydroxide solution. The resulting precipitate was subjected to drying and subsequent recrystallization from methanol, including activated charcoal treatment. The resulting pure product of 2-chloromethyl benzimidazole manifested as slightly yellow-colored crystals.

Subsequently, a mixture of the synthesized 2-chloromethyl benzimidazole (0.01 mol), a substituted amine/alcohol (0.01 mol), and KI (0.01 mol) in 50 ml of ethanol was subjected to reflux for 6 h at 78°C. Dropwise addition of KOH (0.01 mol in 5 ml of water) was carried out under continuous stirring for 2–3 h at room temperature. (Fig. A1). The reaction mixture was then poured into crushed ice, and the resulting solid was separated through filtration, followed by recrystallization from ethanol and subsequent drying in a vacuum desiccator [33].

2.1.1.1. N-[(1H-benzimidazol-2-yl)-methyl]-4-methoxyaniline (B1). Yield: 80 %, R_f: 0.75, m.p: 154–155 °C. FTIR (cm^{-1}): 3210 (N–H), 3000 (sp^2CH), 1640 (C]C), 1585 (C]N), 1200 (C–N). ^{1}HNMR (DMSO, 300 MHz) ppm: 7.13–7.54 (m, 8H, Ar–H), 6.65 (s, 1H, NH benzimidazole), 4.46 (s, 2H, CH_2), 3.61 (s, 3H, OCH_3).^{13}C NMR (DMSO, 100 MHz) ppm: 153.1 (C2), 138 (C4), 137.2 (C5), 114.7 (C6), 123.1 (C7), 122.4 (C8), 116.2 (C9), 47.1 (C10), 147.9 (C12), 114.9 (C13, C16), 114.6 (C14, C17), 157.1 (C15), 56.1 (C18). Elemental analysis: $C_{15}H_{15}N_3O$ (253.29); Calculated; C 71.13, N 16.59, H 5.97 %, Found; C 71.11, N 15.87, H 5.90 %.

2.1.1.2. 4-{[(1H-Benzimidazol-2-yl)-methyl]-amino}-benzoic acid (B2). Yield: 65 %, R_f: 0.82, m.p: 165–166 °C. FTIR (cm^{-1}): 3200 (OH), 3090 (NH), 3050 (sp^2CH), 1715 (C]O), 1670 (C]C), 1550 (C]N), 1250 (C–N). ^{1}HNMR (DMSO, 300 MHz) ppm: 10.58 (s, H, COOH), 7.60–7.86 (m, 8H, Ar–H), 6.45 (s, 1H, NH benzimidazole), 4.69 (s, 2H, CH_2).^{13}C NMR (DMSO, 100 MHz) ppm: 152.8 (C2), 138.1 (C4), 137.4 (C5), 114.5 (C6), 123(C7, C8), 116 (C9), 46.1 (C10), 112.3 (C12, C15), 131.8 (C13, C16), 124.1 (C14), 169.1 (C17). Elemental analysis: $C_{15}H_{13}N_3O_2$ (267.28); Calculated; C 67.40, N 15.72, H 4.90 %, Found; C 67.35, N 15.27, H 4.75 %.

2.1.1.3. 4-{[(1H-Benzimidazol-2-yl)-methyl]-amino}-2-hydroxybenzoic acid (B3). Yield: 70 %, R_f: 0.62, m.p: 156–157 °C. FTIR (cm^{-1}): 3350 (O–H), 3200 (N–H), 3040 (sp^2CH), 1720 (C]O), 1650 (C]C), 1560 (C]N), 1200 (C–N). ^{1}HNMR (DMSO, 300 MHz) ppm: 11.57 (s, 1H, COOH), 7.21–7.66 (m, 7H, Ar–H), 6.70 (s, 1H, NH benzimidazole), 5.41 (s, 1H, OH), 4.60 (s, 2H, CH_2).^{13}C NMR (DMSO, 100 MHz) ppm: 153.2 (C2), 137.7 (C4), 137.2 (C5), 113.9 (C6), 121.9 (C7, C8), 116.2 (C9), 46.1 (C10), 144.7 (C11), 101.1 (C12), 162.9 (C13), 99.9 (C14), 132.1 (C15), 116.1 (C16), 99.8 (C17).Elemental analysis: $C_{15}H_{13}N_3O_3$ (283.28); Calculated; C 63.60, N 14.83, H 4.63 %, Found; C 63.58, N 14.80, H 4.55 %.

2.1.1.4. N-[(1H-Benzimidazol-2-yl)-methyl]-pyridin-2-amine (B4). Yield: 60 %, R_f: 0.79, m.p: 178–179 °C. FTIR (cm^{-1}): 3250 (NH), 3020 (sp^2CH), 1620 (C]C), 1570 (C]N), 1300 (C–N). ^{1}HNMR (DMSO, 300 MHz) ppm: 7.43–8.06 (m, 8H, ArH), 6.35 (s, 1H, NH benzimidazole), 4.44 (s, 2H, CH_2).^{13}C NMR (DMSO, 100 MHz) ppm: 151.9 (C2), 138.2 (C4), 137.2 (C5), 114.5 (C6), 121.9 (C7, C8), 116.2 (C9), 47.1 (C10), 158.2 (C11), 147.9 (C13), 118.7 (C14), 138.1 (C15), 108.1 (C16).Elemental analysis: $C_{13}H_{12}N_4$ (224.26); Calculated; C 72.56, N 22.57, H 4.87 %, Found; C 72.10, N 21.97, H 4.78 %.

2.1.1.5. 2-[(Morpholin-4-yl)-methyl]-1H-benzimidazole (B5). Yield: 60 %, R_f: 0.80, m.p: 162–163 °C. FTIR (cm^{-1}): 3290 (N–H), 3040 (sp^2CH), 1665 (C]C), 1550 (C]N), 1150 (C–N). ^{1}HNMR (DMSO, 300 MHz) ppm: 7.20–7.52 (m, 4H, Ar–H), 6.59 (s, 1H, NH benzimidazole), 4.34 (s, 2H, CH_2), 3.45–3.70 (m, 8H, morpholine-H).^{13}C NMR (DMSO, 100 MHz) ppm: 153.1 (C2), 138.2 (C4), 137.1 (C5), 115.1 (C6), 123.1 (C7, C8), 116.2 (C9), 66.5 (C13, C14), 53.5 (C10), 54.1 (C12, C15), Elemental analysis: $C_{12}H_{15}N_3O$ (217.27); Calculated; C 66.34, N 19.34, H 6.96 %, Found; C 66.27, N 19.30, H 6.88 %.

2.1.1.6. N-[(1H-benzimidazol-2-yl)-methyl]-cyclohexanamine (B6). Yield: 55 %, R_f: 0.75, m.p: 160–161 °C. FTIR (cm^{-1}): 3210 (N–H), 3015 (sp^2CH), 1670 (C]N), 1665 (C]C), 1260 (C–N). ^{1}HNMR (DMSO, 300 MHz) ppm: 7.16–7.44 (m, 4H, Ar–H), 6.69 (s, 1H, NH benzimidazole), 4.38 (s, 2H, CH_2), 2.50 (s, 1H, cyclohexyl H), 1.28–1.78 (m, 10H, cyclohexyl H).^{13}C NMR (DMSO, 100 MHz) ppm: 152.6 (C2), 138.3 (C4), 137.1 (C5), 114.9 (C6), 122.5 (C7, C8), 116.2 (C9), 45.7 (C10), 56.8 (C11), 33.9 (C12, C16), 24.8 (C13, C15), 25.5 (C14). Elemental analysis: $C_{14}H_{19}N_3$ (229.32); Calculated; C 73.33, N 18.32, H 8.35 %, Found; C 72.99, N 18.30, H 8.12 %.

2.1.1.7. N-{4-[(1H-benzimidazol-2-yl)-methoxy]-phenyl}-acetamide (B7). Yield: 70 %, R_f: 0.76, m.p: 169–170 °C. FTIR (cm^{-1}): 3220 (N–H), 3035 (sp^2CH), 1675 (C]O), 1635 (C]C), 1580 (C]N), 1270 (C–N). ^{1}HNMR (DMSO, 300 MHz) ppm: 7.23–7.74 (m, 9H, Ar–H), 6.67 (s, 1H, NH benzimidazole), 4.01 (s, 2H, CH_2), 3.85 (s, 3H, OCH_3).^{13}C NMR (DMSO, 100 MHz) ppm: 155.3 (C2), 137.5 (C4), 137.4 (C5), 114.2 (C6), 122.5 (C7, C8), 116.1 (C9), 70.1 (C10), 158.9 (C11), 114.7 (C12, C16), 122.2 (C13, C15), 133.7 (C14), 169.1 (C17), 24.2 (C18).Elemental analysis: $C_{13}H_{12}N_4$ (281.31); Calculated; C 68.31, N 14.94, H 5.37 %, Found; C 68.12, N 14.85, H 5.25 %.

2.1.1.8. 2-[(pyrrolidin-1-yl)-methyl]-1H-benzimidazole (B8). Yield: 75 %, R_f: 0.72, m.p: 177–178 °C. FTIR (cm^{-1}): 3280 (N–H), 3030 (sp^2CH), 1630 (C]C), 1580 (C]N), 1280 (C–N).^{1}HNMR (DMSO, 300 MHz) ppm: 7.13–7.54 (m, 4H, Ar–H), 6.25 (s, 1H, NH benzimidazole), 4.56 (s, 2H, CH_2), 1.89–2.50 (m, 8H, pyrrolidine-H).^{13}C NMR (DMSO, 100 MHz) ppm: 153.4 (C2), 138.1 (C4), 137.2 (C5), 114.5 (C6), 122.7 (C7, C8), 116.1 (C9), 53.9 (C10), 53.5 (C12, C15), 23.7 (C13, C14). Elemental analysis: $C_{12}H_{15}N_3$ (201.27); Calculated; C 71.61, N 20.88, H 7.51 %, Found; C 71.23, N 20.45, H 7.42 %.

2.2. Anti-inflammatory assays

Anti-inflammatory activity was performed using in vitro oxidative burst assay and in vivo carrageenan induced paw edema method.

2.2.1. In vitro oxidative burst assay using chemiluminescence technique

The Luminol-enhanced chemiluminescence assay [34], was conducted. Briefly, 25 μL of diluted whole blood in Hanks Balanced Salt Solution with calcium chloride and magnesium chloride (HBSS++) [Sigma, St. Louis, USA] was incubated with three different concentrations of compounds (1, 10, and 100 μg/ml), each in triplicate. Control wells received HBSS++ and cells, excluding any compounds. The assay was performed in white half-area 96-well plates [Costar, NY, USA], which were incubated at 37 °C for 15 min in the thermostat chamber of a luminometer [Labsystems, Helsinki, Finland].

Following incubation, 25 μL of serum opsonized zymosan (SOZ) [Fluka, Buchs, Switzerland] and 25 μL of the intracellular reactive oxygen species detecting probe, luminol [Research Organics, Cleveland, OH, USA], were added to each well, excluding blank wells (containing only HBSS++). The levels of reactive oxygen species (ROS) were recorded in the luminometer in terms of relative light units (RLU).

The standard used for the assay was Ibuprofen with an IC50 value of 11.2 ± 1.00.

2.2.2. In vivo carrageenan induced mice paw edema method

The assessment of the anti-inflammatory potential of compounds B2, B4, and B8 was conducted through a carrageenan-induced paw edema model [35]. Mice, following a 12-h fast, were randomly assigned to three groups. Group I served as the negative control, receiving a saline solution (10 ml/kg). Group II received a dose of each compound (10 mg/ml), while Group IV was designated as the positive control, administered diclofenac sodium (10 mg/kg). Subplantar injection of 0.1 ml of 1 % carrageenan solution induced acute paw edema, and treatment commenced 30 min thereafter. Changes in paw volume were monitored at 0, 1, 2, 3, and 4 h post-carrageenan injection using a plethysmometer.

The recorded values were calculated as Mean ± SEM, and statistical significance was determined by comparing p values against the saline group using one-way ANOVA with post-hoc Tukey test. Additionally, percentage inhibition was computed for each compound at each hourly interval.

2.3. Computational analysis

This study incorporates several steps that are described in detail in the next sections. Briefly, the most significant protein families with respect to their roles in inflammatory responses were included in the structure based computational docking of synthesized compounds along with the reference non-steroidal anti-inflammatory and co-crystallized compounds. Synthesized and reference

Table 1
Structures used in this study.

Protein Family	Protein PDB ID	Structure Title	Ligand	Specie	Box Dimensions	Box Volume (A3)	Outer Contour Volume (A3)	Ref
COX-2	3LN1	Structure of Celecoxib bound at the COX-2 active site	Celecoxib	*Musmusculus*	25.00-19.33-20.33	9827	3956	(Wang et al., 2010)
	3PGH	Cyclooxygenase-2 (prostaglandin synthase-2) complexed with a non-selective inhibitor, Flurbiprofen	Flurbiprofen	*Musmusculus*	25.43-21.17-21.63	11,646	4527	(Kurumbail et al., 1996)
	4PH9	The structure of Ibuprofen bound to cyclooxygenase-2	Ibuprofen	*Musmusculus*	24.33-21.33-20.5	10,641	4622	(Harman et al., 2007; Selinsky et al., 2001)
	4COX	Cyclooxygenase-2 (prostaglandin synthase-2) complexed with a non-selective inhibitor, Indomethacin	Indomethacin	*Musmusculus*	26.00-20.00-22.67	11,786	5268	(Kurumbail et al.)
COX-1	1EQH	The 2.7 Å model of ovine cox-1 complexed with Flurbiprofen	Flurbiprofen	*Ovisaries*	19.67-22.17-22.5	9808	4727	(Rimon et al., 2010)
	2OYE	Indomethacin-(R)-alpha-ethyl-ethanolamide bound to Cyclooxygenase-1	Indomethacin-(R)-alpha-ethyl-ethanolamide	*Ovisaries*	22.33-22.50-22.33	11,222	6984	(Xu et al., 2014)
	3KK6	Crystal Structure of Cyclooxygenase-1 in complex with Celecoxib	Celecoxib	*Ovisaries*	18.00-24.00-24.67	10,656	4900	(Singh et al., 2006)
	4O1Z	Crystal Structure of Ovine Cyclooxygenase-1 Complex with Meloxicam	Meloxicam	*Ovisaries*	21.00-20.00-23.33	9799	3108	(Singh et al., 2004)
AKR1C2	4JQ4	AKR1C2 complex with indomethacin	indomethacin	*Homo sapiens*	20.24-31.60-21.53	13,774	10,465	To be published by Authors
	4JTQ	AKR1C2 complex with flurbiprofen	flurbiprofen	*Homo sapiens*	21.16-32.42-24.03	16,484	12,692	
	4JTR	AKR1C2 complex with ibuprofen	ibuprofen	*Homo sapiens*	20.15-31.30-21.97	13,856	10,883	
PLA2	2B17	Specific binding of non-steroidal anti-inflammatory drugs (NSAIDs) to phospholipase A2: Crystal structure of the complex formed between phospholipase A2 and diclofenac at 2.7 A resolution:	diclofenac	*Daboiarusselii*	16.66-13.88-14.73	3406	3335	(Urzhumtsev et al., 1997)
	2DPZ	Structure of the complex of phospholipase A2 with N-(4-hydroxyphenyl)- acetamide at 2.1 A resolution	N-(4-hydroxyphenyl)-acetamide (Tylenol)	*Daboiarusselii*	17.33-16.00-14	3397	3071	(Steuber, 2011)
AR	1AH3	Aldose reductasecomplexed with Tolrestat inhibitor	Tolrestat	*Susscrofa*	26.56-34.38-19.09	17,427	11,880	(Brownlee et al., 2006)
	3U2C	Aldose reductase in complex with NSAID-type inhibitor at 1.0 A resolution	Sulindac	*Homo sapiens*	37.12-21.35-24.81	19,656	13,508	(Steuber, 2011)
	2INZ	Crystal Structure of Aldose Reductasecomplexed with 2-Hydroxyphenylacetic Acid	(2-Hydroxyphenyl) Acetic Acid	*Homo sapiens*	25.20-21.12-34.43	18,325	12,017	(Rimon et al., 2010)

compounds were later on docked in the selected protein targets using different modules of docking provided by OpenEye scientific software (www.eyesopen.com). Docking was performed using two different strategies including FRED 3.2.0.2 [36] and HYBRID 3.2.0.2 [37]: OpenEye Scientific Software, Santa Fe, NM. (http://www.eyesopen.com). Each docked compound was energy minimized in the docked sites to reduce the steric hindrances. Next, the docking methods were verified by the pose analysis of co-crystallized ligands with the re-docked conformations. Finally ligand poses were analyzed against their overall ligand-protein interaction terms.

Table 2
Characterization data of the synthesized benzimidazole derivatives B1–B8.

S	Yield (%)	R_f	m.p (°C)	Molecular structure
B1	80	0.75	154	$C_{15}H_{15}N_3O$
B2	65	0.82	165	$C_{15}H_{13}N_3O_2$
B3	70	0.72	156	$C_{15}H_{13}N_3O_3$
B4	60	0.79	178	$C_{13}H_{12}N_4$
B5	60	0.8	162	$C_{12}H_{15}N_3O$
B6	55	0.71	160	$C_{14}H_{19}N_3$
B7	75	0.7	169	$C_{16}H_{15}N_3O_2$
B8	70	0.75	177	$C_{12}H_{15}N_3$

2.3.1. Protein targets

Table 1 shows the complete information about the selected proteins used in this study. All of these proteins are members of those protein families which have their significant role in mediating inflammatory responses. These proteins were prepared using the Make Receptor 3.2.0.2 software of OpenEye (OpenEye software (www.eyesopen.com).

2.3.2. Ligand selection and preparation

Synthesized compounds i.e. B1–B8 along with already FDA approved NSAIDS and Co-crystallized compounds were selected for docking based on their significant roles in regulating inflammatory responses. Selected twenty-five ligands used in this study are shown in Fig. A2. Interconversion of file formats and 2D depictions of compounds were generated using Open Babel software. Hierarchal Clustering of molecules is performed using the JOELIB descriptors in Chemmine tools [38](Fig. A3). The descriptors with null values were not considered during clustering. The molecules were subjected to protonation, charge and pKa fixation along with their tautomers generation using QUACPAC 1.7.0.2: OpenEye Scientific Software, Santa Fe, NM. (http://www.eyesopen.com). Further conformations of all molecules were generated with a maximum size of 2000 in OMEGA 2.5.1.4: OpenEye Scientific Software, Santa Fe, NM. http://www.eyesopen.com [39]. SZYBKI 1.9.0.3: OpenEye Scientific Software, Santa Fe, NM (http://www.eyesopen.com) was used to energy minimized the conformations of all molecules.

2.3.3. Grid selection

Molecular cavities containing co-crystallized inhibitors were considered for docking in each protein except for protein structures of AKR1C2 and AR protein families. In these structures, the inhibitor and NADP molecules were both selected to make the grid for docking due to the small distance of $<5°$A between them which makes a channel for the active sites. The box was placed around the co-crystallized ligand in such a manner that the box should cover maximum possible solvent exposed area around the active site without compromising the other dimensions. The dimensions and volume of the contour maps of each protein are provided in Table 1. The shape of outer contour was selected in such a manner that it should completely fill the box and extend towards the solvent. Auto generated constraints were not considered during structure preparation.

2.3.4. Docking

Computational docking of compounds in the specified grids made for each protein was performed using FRED 3.2.0.2 and HYBRID 3.2.0.2 OpenEye Scientific Software, Santa Fe, NM. (http://www.eyesopen.com) [36,37],with the 94s variant of Merck Molecular Force Field (MMFF94s) and Chemgauss4 scoring function. This two software were used separately to validate the poses of compounds inside the active site. SZYBKI 1.9.0.3: OpenEye Scientific Software, Santa Fe, NM. (http://www.eyesopen.com) was used to minimize the docked molecules in the active site. Several poses and tautomeric states of each ligand were used for subsequent analysis. Visual analysis of the binding modes was performed in VIDA 4.3.0.4: OpenEye Scientific Software, Santa Fe, NM. (http://www.eyesopen.com).

3. Results and discussion

3.1. Physicochemical studies

TLC was performed on TLC plates. Mobile phase: ethyl acetate: petroleum ether (1:2). The plates were developed in closed chromatography tanks saturated with the mobile phase at 24 °C. Spots were detected under UV light or by iodine vapors. R_f values were calculated by formula R_f = distance travelled by sample/distance travelled by solvent front. Results are illustrated in Table 2.

The Rf values, indicative of the compounds' mobility in chromatographic systems, range from 0.70 to 0.82. These values provide insights into the compounds' polarity and interactions with the stationary phase during chromatographic separation. Compounds with higher Rf values tend to exhibit greater mobility and may elute earlier in chromatographic analyses.

The melting points (m.p) of the synthesized compounds vary from 154 °C to 178 °C. These values represent the temperature range

Table 3
In vitro anti-inflammatory activity of benzimidazole derivatives B1–B8 using Oxidative burst assay.

S	Concentration (μg/ml)	IC_{50}±SD
B1	1, 10, 100	21.8 ± 1.2
B2	1, 10, 100	4.6 ± 1.4
B3	25	–
B4	1, 10, 100	2.4 ± 0.2
B5	25	–
B6	25	–
B7	1, 10, 100	11.2 ± 1.7
B8	1, 10, 100	5.4 ± 1.0
Ibuprofen	25	11.2 ± 1.9

at which the compounds transition from solid to liquid phases, providing information about their molecular packing and purity. Consistent melting points within narrow ranges suggest high degrees of molecular homogeneity and crystallinity, which are desirable characteristics for many applications.

The molecular structures of the compounds, represented by their empirical formulas, highlight the diversity in chemical compositions and functional group arrangements. Structural variations among the compounds contribute to their distinct physical and chemical properties, influencing their potential applications in pharmaceutical.

3.2. Chemistry

All the benzimidazole derivatives B1–B8 were synthesized by the reaction of appropriate amines with 2-chloromethyl benzimidazole. Characterization was done by FTIR, ^{1}HNMR, ^{13}CNMR and elemental analysis data. In IR spectra NH and C]C stretchings were observed for all the compounds. Additionally carbonyl stretchings were present in B2, B3 and B8. ^{1}HNMR data confirmed the formation of target compounds. The characteristic protons of methylene group appeared at 4.01–4.69 ppm in all compounds. In B2 singlet of OH was observed at 5.41 ppm while in B5, B6 and B7 the aliphatic protons resonated as multiplets in the upfield region. ^{13}CNMR and elemental analysis data also supported the formation of target compounds B1–B8.

The results of the compounds B1 to B8 provide a detailed overview of their synthesis and characterization, showcasing a range of chemical functionalities and structural variations. Across the compounds, common peaks in spectroscopic data include those indicative of aromatic and heterocyclic moieties, such as peaks corresponding to sp2CH bonds, C]C bonds, and N–H bonds. These peaks are consistent with the presence of benzimidazole or related aromatic systems within the molecules. Additionally, peaks associated with specific functional groups like C–N bonds and C]O bonds are observed, providing further insights into the molecular structures. However, variations exist in the spectra, with some compounds exhibiting additional peaks corresponding to unique functional groups, such as OH or COOH groups in B2 and B3, respectively.

The yields of the synthesized compounds also vary, ranging from 55 % to 80 %. While some compounds achieve relatively high yields, others have lower yields, potentially indicating differences in reaction efficiencies or purification challenges. Factors such as the complexity of the synthetic route, the stability of intermediates, and the effectiveness of purification techniques can influence yield variations among the compounds. Despite differences in yields, the successful synthesis of multiple compounds demonstrates the effectiveness of the synthetic strategies employed. These initial findings represent a starting point, and we recognize the need for further method development to enhance yields. We are committed to advancing our research and refining our methodologies to achieve higher yields in subsequent stages. Therefore, while the current yields may be suboptimal, we are dedicated to optimizing our processes to ensure the potential benefits of these novel compounds can be realized in future developmental stages.

Comparing the common and uncommon peak ranges across the compounds provides valuable insights into the structural diversity and functional group modifications achieved in this synthetic series. Such variations in chemical structure and functional groups are crucial for exploring the potential biological or material properties of these compounds. Overall, these results underscore the importance of comprehensive characterization in understanding the chemical properties and potential applications of synthesized compounds, while also highlighting the significance of optimizing synthetic methodologies to achieve higher yields and purities.

3.3. In vitro anti inflammatory activity

All the synthesized derivatives of benzimidazole were evaluated for their in vitro anti-inflammatory activity using oxidative burst assay. The standard inhibitor used was ibuprofen (IC_{50} = 11.2 ± 1.9 μg/ml). Among all the compounds B1, B2, B4, B7 and B8 showed prominent activity with IC_{50} values of 2.4 ± 0.2 to 21.8 ±0 .1.2. Highest anti-inflammatory activity was shown by compound B4 (IC_{50} = 2.4 ± 0.2 μg/ml) having aminopyridine moiety. Compound B2 having COOH group also exhibited better activity (IC_{50} of 4.6 ± 1.4 μg/ml) as compared to standard drug. Third maximum anti-inflammatory activity was shown by B8 (IC_{50} = 5.4 ± 1.0 μg/ml) due to the presence of pyrrolidine moiety. Paracetamol containing benzimidazole derivative B7 showed activity (IC_{50} = 11.2 ± 1.7 μg/ml) comparable to that of standard. In case of compounds B3, B5 and B6, the activity was not significant at 25 μg/ml (Table 3).

Table 4
Anti-inflammatory effect against carrageenan paw edema by B2, B4 and B8.

S	0 h	1 h	2 h	3 h	4 h
Control (Saline 10 ml/kg)	0.35 ± 0.005	0.41 ± 0.005	0.45 ± 0.005	0.52 ± 0.003	0.51 ± 0.005
B2 (10 mg/kg)	0.30 ± 0.008**	0.27 ± 0.008*** 34 %	0.23 ± 0.011*** 48 %	0.23 ± 0.011*** 56 %	0.23 ± 0.01*** 55 %
B4 (10 mg/kg)	0.29 ± 0.004***	0.237 ± 0.011*** 42 %	0.192 ± 0.007*** 57 %	0.177 ± 0.004*** 66 %	0.177 ± 0.004*** 65 %
B8 (10 mg/kg)	0.26 ± 0.01***	0.26 ± 0.005*** 37 %	0.22 ± 0.006*** 51 %	0.19 ± 0.005*** 63.4 %	0.18 ± 0.008*** 65 %
Standard (Diclofenac Sodium 20 mg/kg)	0.35 ± 0.005***	0.32 ± 0.005*** 22 %	0.27 ± 0.005*** 40 %	0.22 ± 0.003*** 58 %	0.16 ± 0.004*** 69 %

Values are shown as Mean ± SEM, n = 5. ***$p < 0.001$, **$p < 0.05$ vs. saline group one-way ANOVA with post-hoc Tukey Test.

3.4. In vivo carrageenan induced mice paw edema method

Compounds B2, B4 and B8 with maximum in vitro anti-inflammatory activity were further investigated for their in vivo potential using carrageenan induced paw edema assay. All the three derivatives showed promising results with marked decrease in paw volume after 0, 1, 2, 3 and 4 h. At the dose of 10 mg/kg, B2 reduced the paw edema from 0.30 ± 0.008 mm at 0 h to 0.23 ± 0.011 mm after 2 h which persisted after 4 h. At the same dose compound B4 decreased the paw edema values to 0.29 ± 0.004, 0.237 ± 0.011, 0.192 ± 0.007, 0.177 ± 0.004 and 0.177 ± 0.004 mm ($p < 0.001$ vs. saline group) respectively after 0, 1, 2, 3 and 4 h. Compound B8 at the dose of 10 mg/kg reduced the paw edema values to 0.26 ± 0.01, 0.26 ± 0.005, 0.22 ± 0.006, 0.19 ± 0.005 and 0.18 ± 0.008 mm ($p <$ 0.001 vs. saline group) respectively. Both B4 and B8 were found to exhibit maximum inhibition (65 %) slightly lower than the standard. B4 having amino pyridine moiety and B8 with pyrrolidine group were most active probably due to greater lypophilic and basic nature. B2 having COOH group also showed good activity but low as compared to other two due to its greater polarity and acidic nature. Results are shown in Table 4 and graphical representation of the above-mentioned results for compounds B2, B4 and B8 are shown in Fig. A4.

3.5. Computational analysis

Computational studies for docking of synthesized molecules along with the reference compounds were performed in an attempt to rationalize the experimental data.

3.5.1. Validation of docking methodology

Several methods are available for the confirmation and validation of docking methodologies. We selected the re-docking of the co-crystallized molecule in the same protein using different methods used in our study. Fig. A5 shows an example of the poses obtained for flurbiprofen and Ibuprofen which are present as co-crystallized in the protein structures of COX-1 (PDB Id: 1EQH) and COX-2 (PDB Id: 4PH9) using two different docking protocols. Pose analysis validates that the FRED and HYBRID with energy minimizations (referred as FredOpt and HybridOpt in this study) of docked molecules in the protein produced nearly the same conformation as can be seen in the co-crystallized forms.

3.5.2. Docking using FRED with optimization (FredOpt)

The overall distributions of ligand-protein interaction terms obtained by FredOpt for all of the structures and ligands are given in Fig. A6 and Fig. A7, respectively. It can be observed that the best structures or targets are from the families of AR, PLAs, and AIKRC comparative to the COX-1 or 2 family. By looking at the individual ligand-protein terms for each ligand, it can be seen that ligands which are successfully docked by FredOpt in structures have comparatively higher ligand-protein interaction terms in COX-1 and COX-2 as compared to the structures of AR, PLAs, and AIKRC. In COX-2, Tylenol (2dpz Colig), acetaminophen and OHP have the lowest ligand-protein interaction terms whereas the synthesized ligands have shown a positive value. In case of AR, the synthesized ligands have shown much promising results in terms of lower ligand-protein interaction terms. In AR, minimum and small distribution of ligand-protein interaction terms is found significant for the synthesized compounds B2 and B3. In case of AIKRC, synthesized compound B7 has been found with the lowest in terms which is < -15 k/mol. In case of COX-1, all synthesized compounds except B7 were found with positive value. Similar to the AR, in PLA2, synthesized compounds B2 and B3 have been found with the lowest ligand-protein interaction terms compared to the original co-crystallized ligands like Diclofenac (PDB Id: 2B17). This docking protocol provides an instance that the synthesized compounds including B2, B3 and B7 are promising lead molecules for non-cox based anti-inflammatory responses.

3.5.3. Docking using HYBRID with optimization (HybridOpt)

The overall distributions of ligand-protein interaction terms obtained by HybridOpt for all of the structures and individual ligands are given in Fig. A8 and Figures A9, respectively. Comparative to the FredOpt protocol, it can be observed that docking of ligands in the structures have similar ligand-protein interaction terms and significant difference cannot be found. In COX-2, Tylenol (co-crystallized ligand of PDB ID: 2DPZ), acetaminophen and OHP have shown the lowest ligand-protein interaction terms, whereas the synthesized ligands have shown positive values like in case of FredOpt. In case of AR, the synthesized compounds such as B1, B4 along with B2 and B3 having significant negative interaction terms. In case of AIKRC, synthesized compound B3 have significant lower ligand-protein interaction terms. In case of COX-1, all synthesized compounds except B4 were found with positive values showing their non-selective nature towards COX-1. Similar to the FredOpt, in PLA2, synthesized compounds B2 and B3 have been found with the negative values.This docking protocol provides an instance that the synthesized compounds including B1-4 and B7are promising lead molecules for inhibiting AR, PLA2 and AIKRC.

3.5.4. Poses of synthesized ligands

The poses of all compounds with each protein structures have been analyzed and given as Supplementary File 3 (containing prepared structures, FRED and HYBRID docked molecules with and without optimizations). Here, we have discussed and shown the poses of only those synthesized compounds which have significantly lower interaction terms with structures of AIKRC, AR and PLA2.

3.5.4.1. AIKRC. The docked poses of synthesized compounds in structures of AIKRC have been analyzed as shown in Fig. A10. For the comparison, Ibuprofen (blue sticks) and co-crystallized molecules of each structure (light yellow sticks) have also been shown in each case. The most promising binding of synthesized compounds with small distributions of interaction terms across three structures i.e. 4JQ4, 4JTQ and 4JTR are found for B2 and B7 in FredOpt protocol whereas B3 is found with significantly low ligand-protein interaction terms levels in HybridOpt protocol.

3.5.4.2. AR. The docked poses of synthesized compounds in structures of AR have been analyzed. For the comparison, Ibuprofen (blue sticks) and co-crystallized molecules of each structure (light yellow sticks) have also been shown in each case. The most promising binding of synthesized compounds with small distributions of ligand-protein interaction terms across three structures i.e. 1AH3, 2INZ and 3U2C are found for B2-3 in FredOpt protocol as shown in Fig. A11, whereas B1-4 are found with significant ligand-protein interaction terms in HybridOpt protocol.

3.5.4.3. PLA2. The docked poses of synthesized compounds in structures of PLA2 have been analyzed. For the comparison, Ibuprofen (blue sticks) and co-crystallized molecules of each structure (light yellow sticks) have also been shown in each case. The most promising binding of synthesized compounds with small distributions of ligand-protein interaction terms across two structures i.e. 2B1Z and 2DPZ are found for B2-3 in FredOpt and HybridOpt protocols as shown in Fig. A12.

The exploration of the structure-activity relationship (SAR) among the synthesized benzimidazole derivatives sheds light on the nuanced interplay between chemical structure and anti-inflammatory efficacy. Each compound, characterized by distinct chemical moieties and functional groups, exhibited varying degrees of potency in inhibiting inflammatory processes.

Compound B1, distinguished by its methoxy aniline derivative of benzimidazole, demonstrated noteworthy anti-inflammatory activity, establishing a foundation for further investigation into the role of this specific structural motif in mediating biological effects. Its efficacy, reflected in the IC50 values ranging from 2.4 ± 0.2 to 21.8 ± 1.2 μg/ml, underscores the potential significance of methoxy aniline substitution in conferring anti-inflammatory properties to benzimidazole derivatives.

Similarly, compound B2, identified as a 4-amino benzoic acid derivative, displayed significant potency with an IC50 of 4.6 ± 1.4 μg/ml. This observation highlights the potential contribution of the 4-amino benzoic acid moiety to the anti-inflammatory activity of benzimidazole derivatives, suggesting a role for this functional group in modulating pharmacological effects.

The exceptional potency of compound B4, characterized as a pyridine 2 amine derivative, further underscores the importance of structural modifications in enhancing anti-inflammatory efficacy. With an IC50 value of 2.4 ± 0.2 μg/ml, compound B4 emerged as the most potent among the tested compounds, indicating the potential significance of pyridine 2 amine substitution in augmenting the biological activity of benzimidazole derivatives.

Conversely, compounds B3, B5, and B6, incorporating 2-hydroxy 4-amino benzoic acid, morpholine, and cyclohexylamine derivatives, respectively, demonstrated less pronounced activity at 25 μg/ml. This suggests that certain structural modifications may attenuate or modulate the anti-inflammatory effects of benzimidazole derivatives, highlighting the need for further exploration and optimization.

Compound B7, characterized by a 4-methoxy phenylacetamide derivative, exhibited promising anti-inflammatory effects, underscoring the potential contribution of phenylacetamide substitution to biological activity. Similarly, compound B8, identified as a pyrrolidine derivative, displayed significant efficacy, suggesting the importance of pyrrolidine substitution in modulating anti-inflammatory responses.

In summary, the observed variations in anti-inflammatory efficacy among the synthesized benzimidazole derivatives highlight the

complex relationship between chemical structure and pharmacological activity. These findings provide valuable insights into the design and optimization of novel anti-inflammatory agents, paving the way for the development of more effective therapeutic interventions.

Overall, the findings suggest that benzimidazole derivatives hold promise as potent anti-inflammatory agents, with compounds B4 and B8 showing remarkable efficacy in both in vitro and in vivo evaluations. The computational analysis provided valuable insights into their mechanisms of action, highlighting their potential as lead molecules for further exploration in non-COX-based anti-inflammatory drug development. These results underscore the importance of benzimidazole derivatives as promising candidates in the quest for novel anti-inflammatory therapies, warranting further investigation and optimization in preclinical and clinical settings.

4. Conclusion

Despite considerable progress in the identification and development of new anti-inflammatory agents, the exact mechanism of action is still unknown. There are several pathways which are involved in the process of inflammation. This paper outlines the synthesis of new benzimidazole derivatives, their characterization, detailed computational profiling and anti-inflammatory evaluation (*In vitro & In vivo*). The synthesized derivatives showed significant binding potential with selected pathway proteins up to varying degree i.e., COX 2, AR, AIKRC, COX 1, PLAs. The *In vitro* anti-inflammatory analysis predicts B4, B2, B8 and B7 as good agents while In vivo screening showed B4, B8 and B2 as remarkable anti-inflammatory agents. The vital anti-inflammatory potential of the newly synthesized derivatives against several proteins is promising and it will further provide opportunities in the synthesis of new agents as well as to establish its mechanism of action.

Ethics approval and consent to participate

Attached as Supplementary file.

Funding

No Funding.

Consent for publication

Not Applicable.

Availability of data and materials

Available.

CRediT authorship contribution statement

Shaher Bano: Investigation, Data curation. **Humaira Nadeem:** Validation, Supervision, Project administration, Data curation, Conceptualization. **Iqra Zulfiqar:** Software, Investigation. **Tamseela Shahzadi:** Visualization, Formal analysis. **Tayyaba Anwar:** Resources, Project administration. **Asma Bukhari:** Investigation, Data curation. **Syed Muzzammil Masaud:** Writing – review & editing, Writing – original draft, Conceptualization.

Declaration of competing interest

The authors declare that they have no known competing financial interests or personal relationships that could have appeared to influence the work reported in this paper.

Appendix A. Supplementary data

Supplementary data to this article can be found online at https://doi.org/10.1016/j.heliyon.2024.e30102.

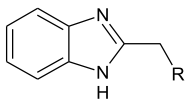

Fig. A1.

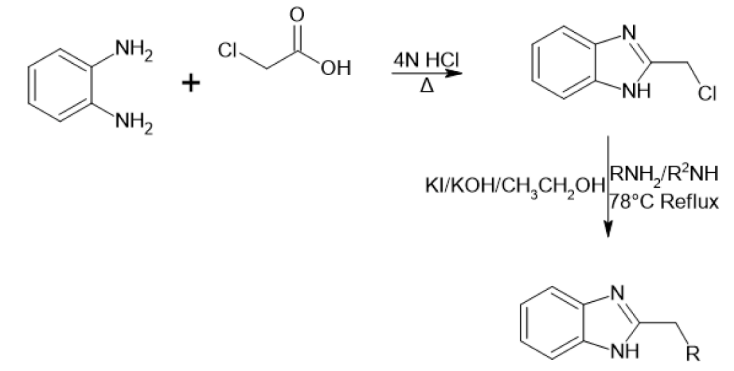

Where R =

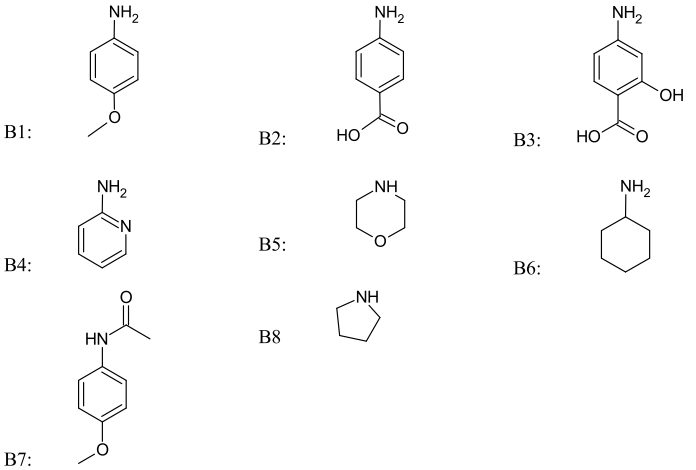

Structures of Synthesized Benzimidazole Derivatives

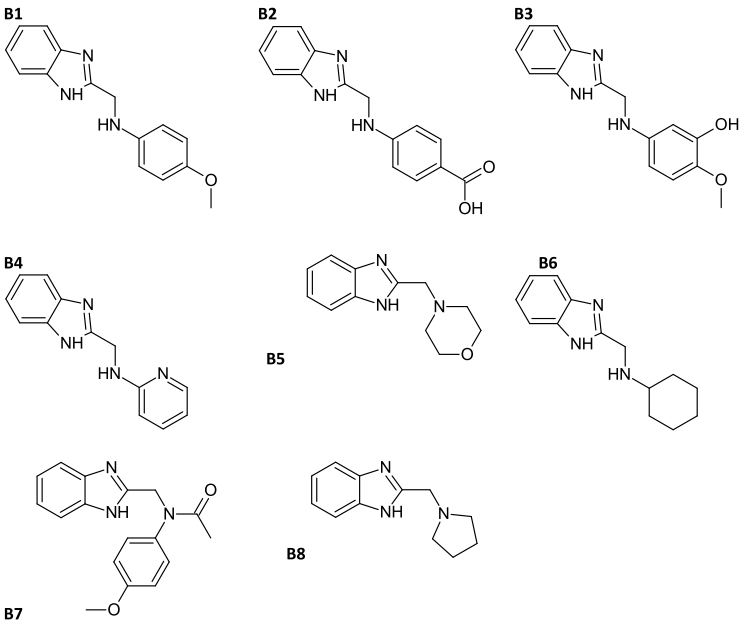

Fig. A2.

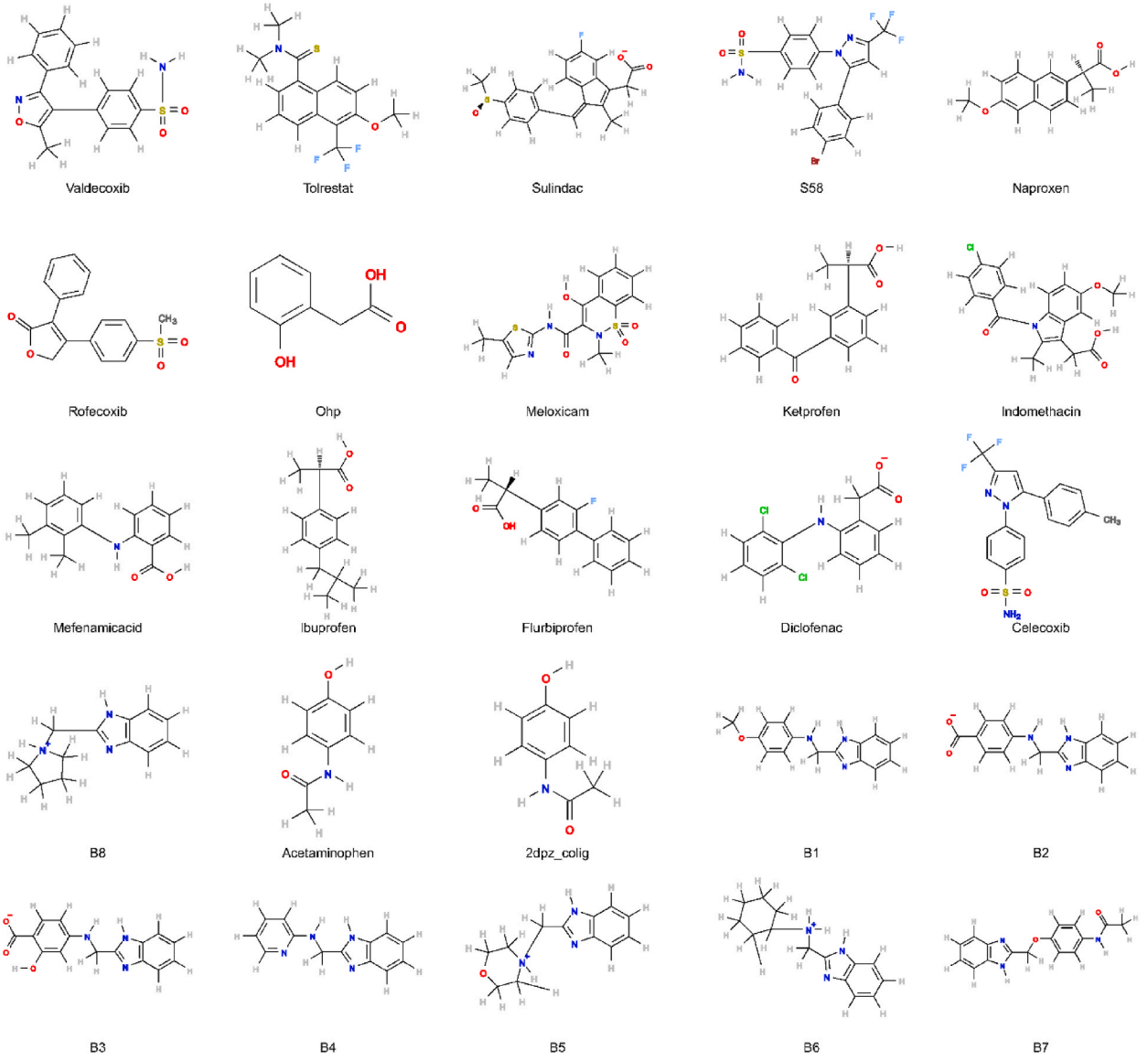
Valdecoxib
Tolrestat
Sulindac
S58
Naproxen
Rofecoxib
Ohp
Meloxicam
Ketprofen
Indomethacin
Mefenamicacid
Ibuprofen
Flurbiprofen
Diclofenac
Celecoxib
B8
Acetaminophen
2dpz_colig
B1
B2
B3
B4
B5
B6
B7

Fig. A3.

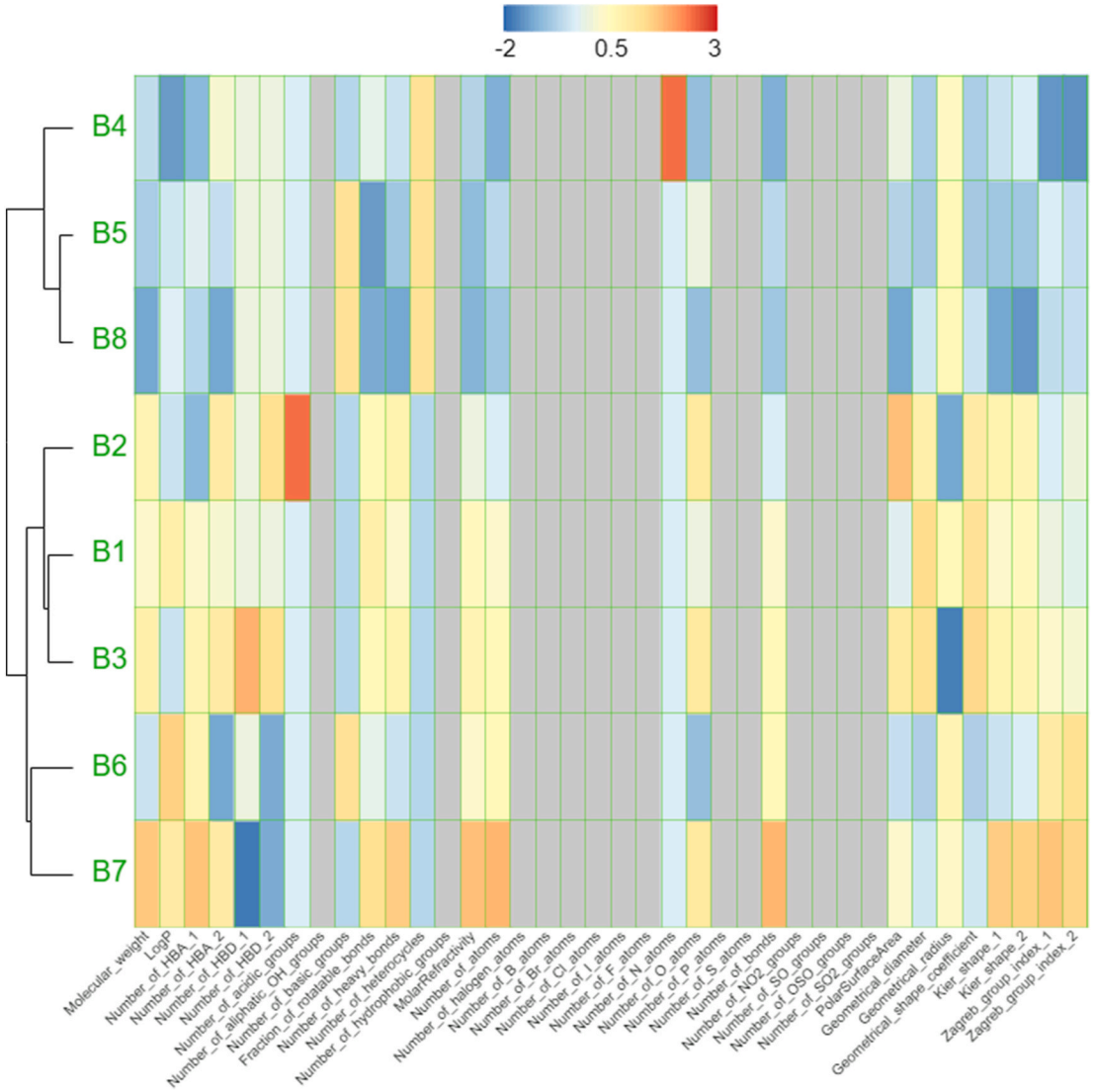
-2
0.5
3
B4
B5
B8
B2
B1
B3
B6
B7
Molecular_weight
LogP
Number_of_HBA_1
Number_of_HBA_2
Number_of_HBD_1
Number_of_HBD_2
Number_of_aliphatic_OH_groups
Number_of_acidic_groups
Number_of_basic_groups
Fraction_of_rotatable_bonds
Number_of_heavy_bonds
Number_of_heterocycles
Number_of_hydrophobic_groups
MolarRefractivity
Number_of_atoms
Number_of_halogen_atoms
Number_of_B_atoms
Number_of_Br_atoms
Number_of_Cl_atoms
Number_of_I_atoms
Number_of_F_atoms
Number_of_N_atoms
Number_of_O_atoms
Number_of_P_atoms
Number_of_S_atoms
Number_of_bonds
Number_of_NO2_groups
Number_of_SO_groups
Number_of_OSO_groups
Number_of_SO2_groups
PolarSurfaceArea
Geometrical_diameter
Geometrical_radius
Geometrical_shape_coefficient
Kier_shape_1
Kier_shape_2
Zagreb_group_index_1
Zagreb_group_index_2

Fig. A4.

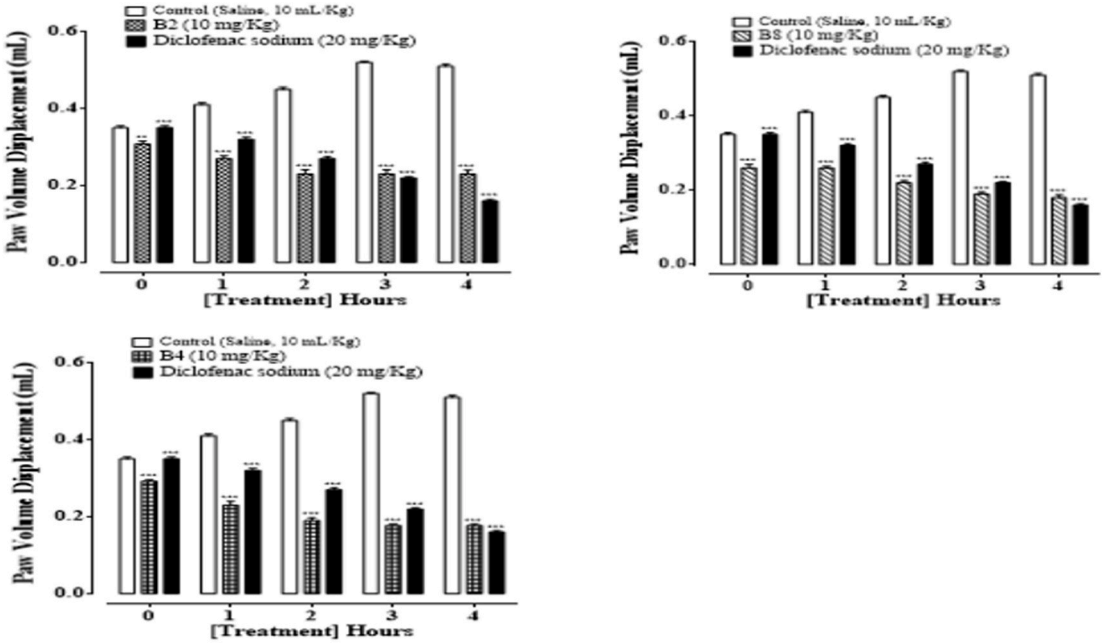
Control (Saline, 10 mL/Kg)
B2 (10 mg/Kg)
Diclofenac sodium (20 mg/Kg)
Paw Volume Displacement (mL)
[Treatment] Hours
Control (Saline, 10 mL/Kg)
B8 (10 mg/Kg)
Diclofenac sodium (20 mg/Kg)
Paw Volume Displacement (mL)
[Treatment] Hours
Control (Saline, 10 mL/Kg)
B4 (10 mg/Kg)
Diclofenac sodium (20 mg/Kg)
Paw Volume Displacement (mL)
[Treatment] Hours

Fig. A5.

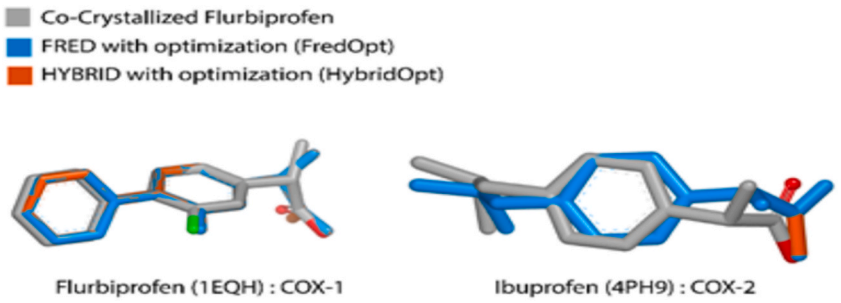
Co-Crystallized Flurbiprofen
FRED with optimization (FredOpt)
HYBRID with optimization (HybridOpt)
Flurbiprofen (1EQH) : COX-1
Ibuprofen (4PH9) : COX-2

Fig. A6.

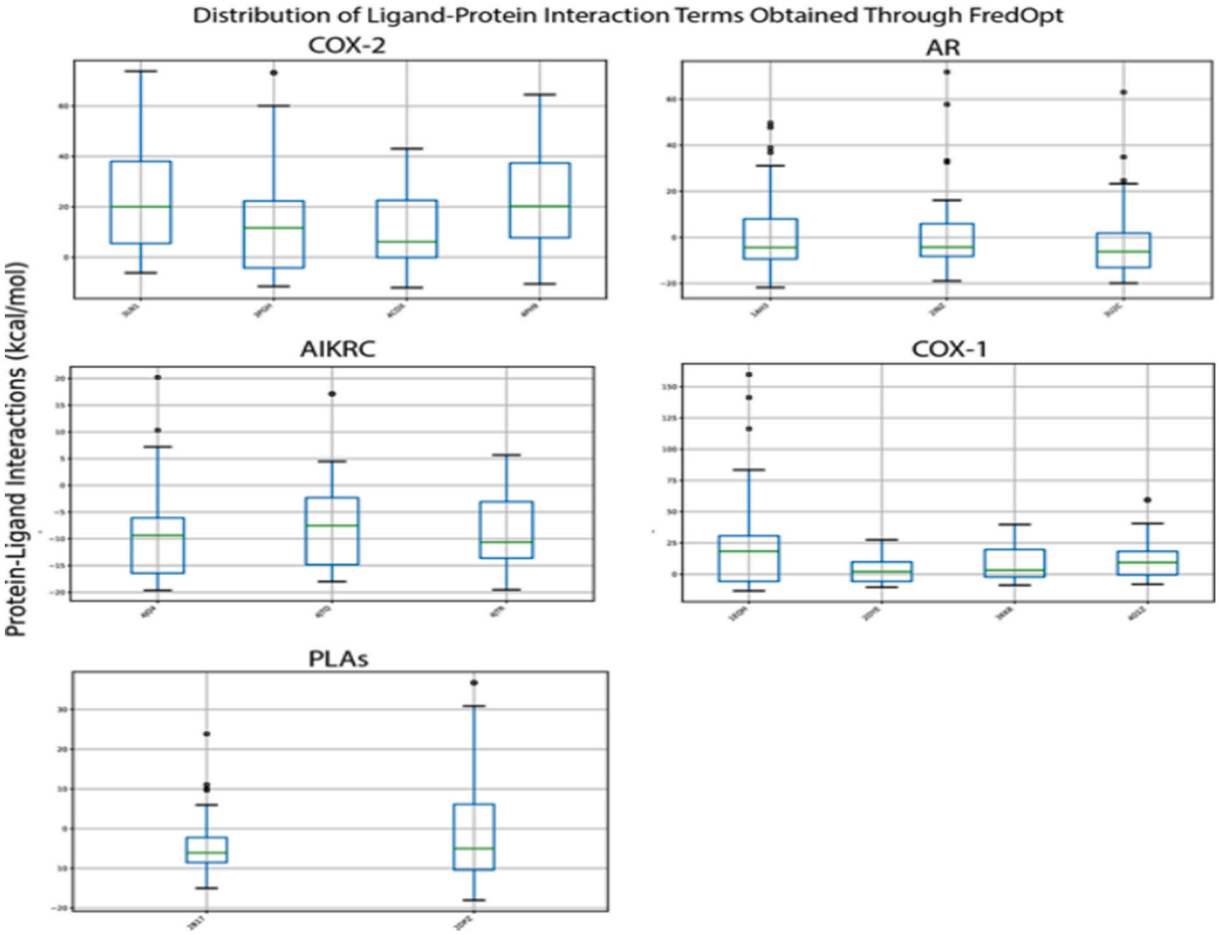
Distribution of Ligand-Protein Interaction Terms Obtained Through FredOpt
COX-2
AR
AIKRC
COX-1
PLAs
Protein-Ligand Interactions (kcal/mol)

Fig. A7.

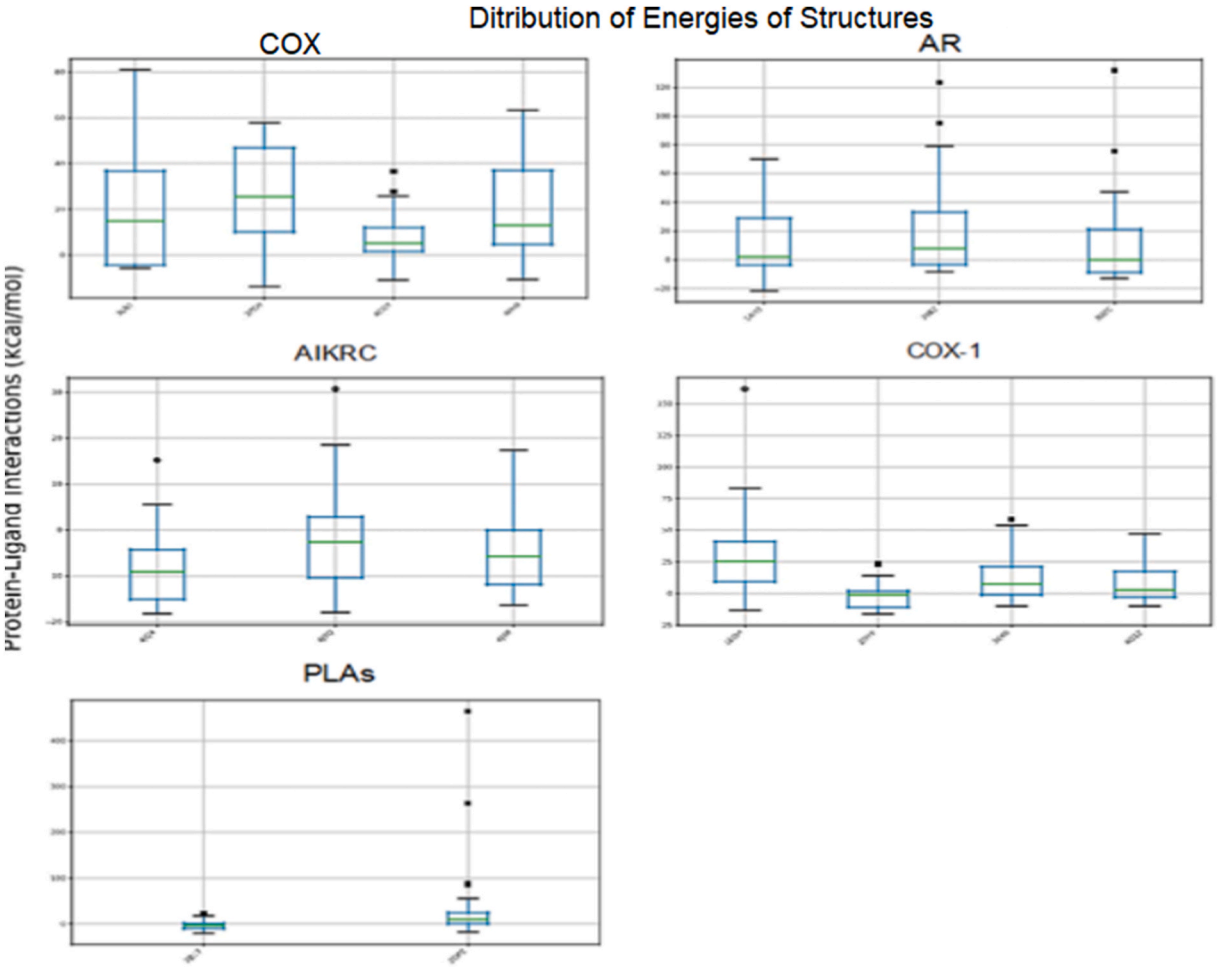
Ditribution of Energies of Structures
COX
AR
AIKRC
COX-1
PLAs
Protein-Ligand Interactions (kcal/mol)

Fig. A8.

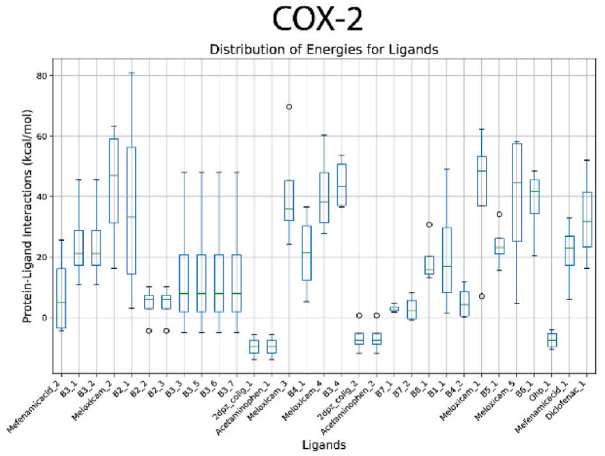
COX-2
Distribution of Energies for Ligands
Protein-Ligand Interactions (kcal/mol)
Ligands

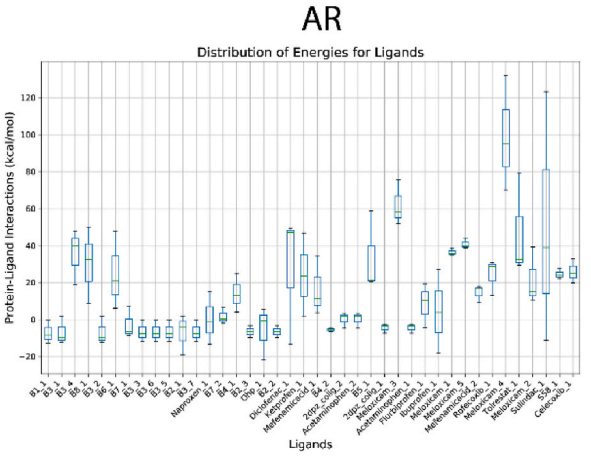
AR
Distribution of Energies for Ligands
Protein-Ligand Interactions (kcal/mol)
Ligands

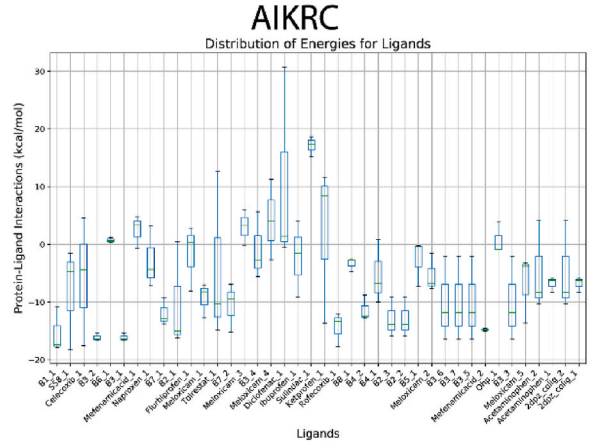
AIKRC
Distribution of Energies for Ligands
Protein-Ligand Interactions (kcal/mol)
Ligands

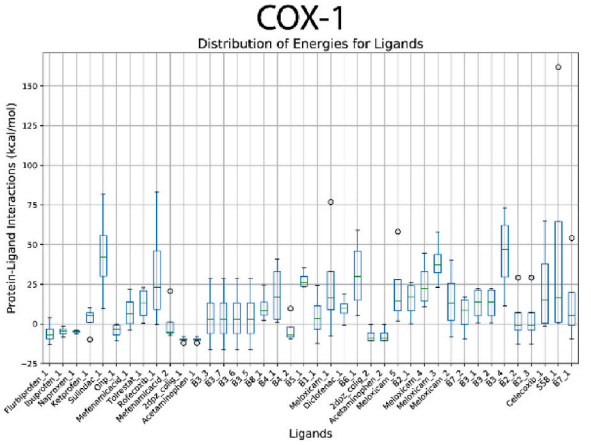
COX-1
Distribution of Energies for Ligands
Protein-Ligand Interactions (kcal/mol)
Ligands

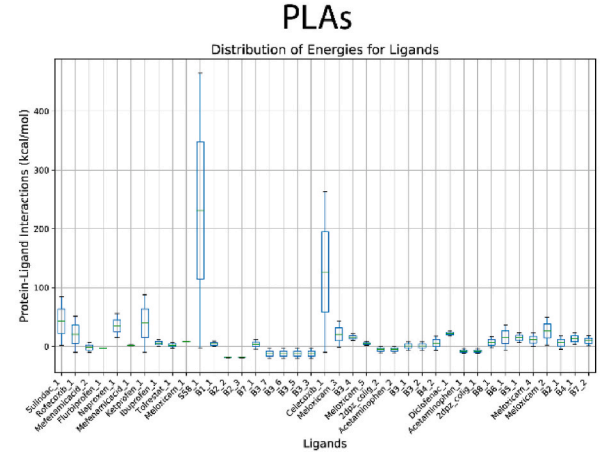
PLAs
Distribution of Energies for Ligands
Protein-Ligand Interactions (kcal/mol)
Ligands

Fig. A9.

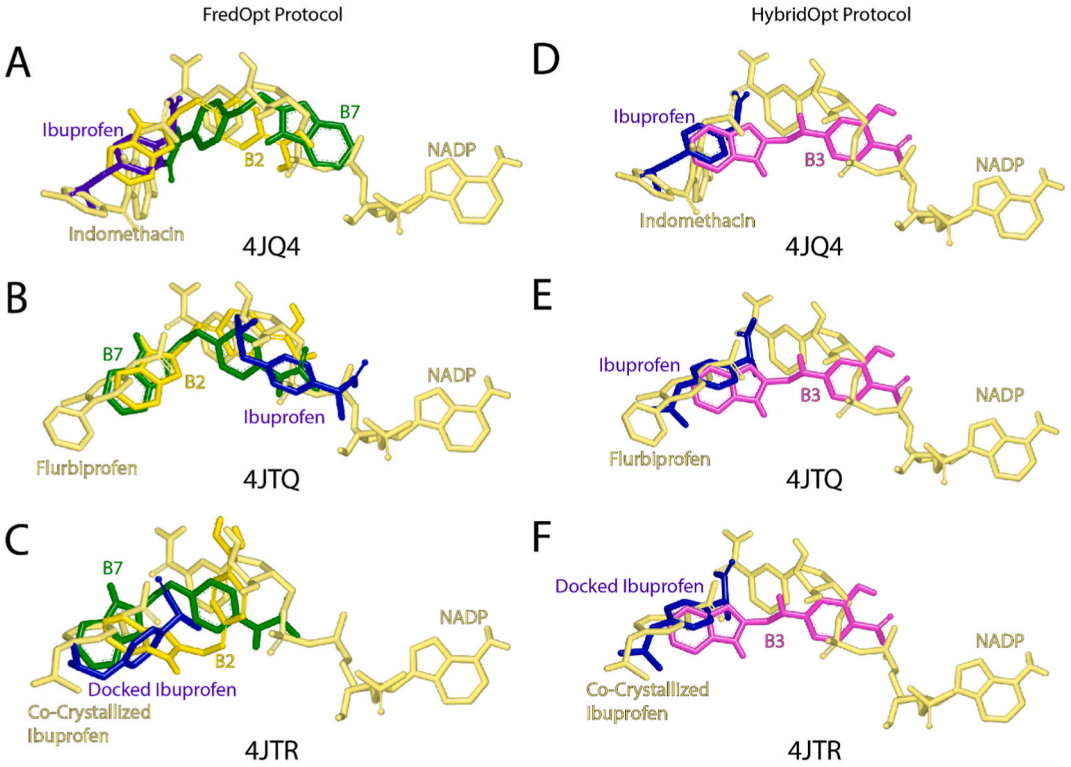

Fig. A10.

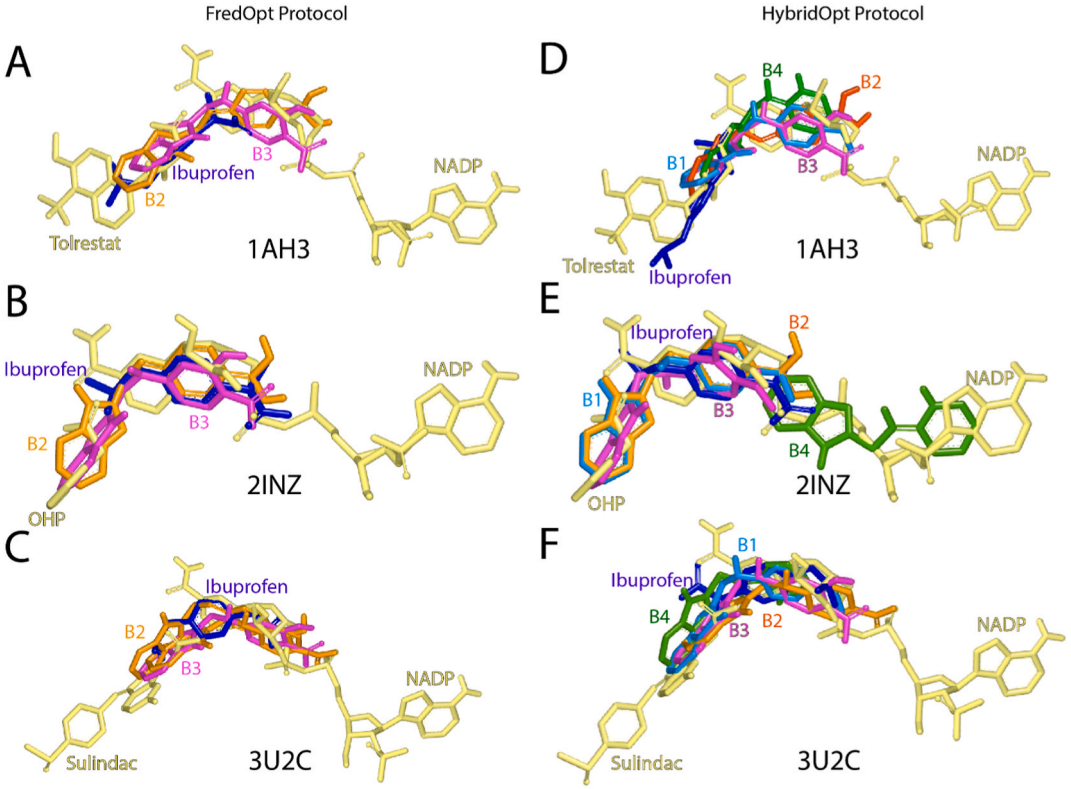

Fig. A11.

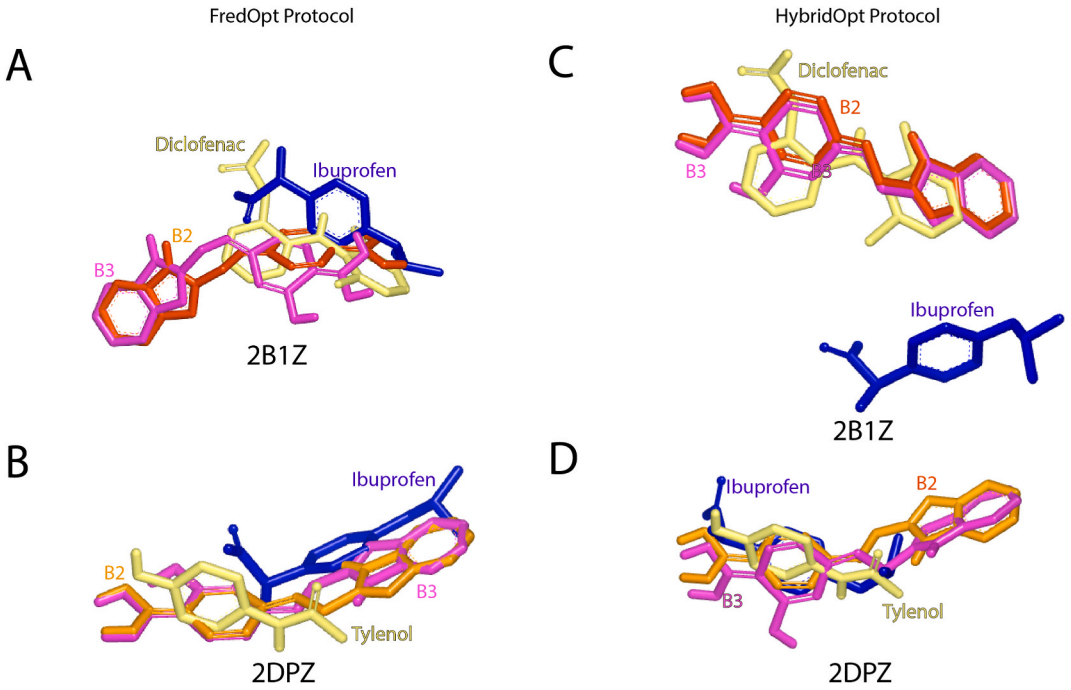

Fig. A12.

References

[1] G. Singh, Gastrointestinal complications of prescription and over-the-counter nonsteroidal anti-inflammatory drugs: a view from the ARAMIS database, Am. J. Therapeut. 7 (2) (2000) 115–122, https://doi.org/10.1097/00045391-200007020-00008.

[2] W. Pruzanski, P. Vadas, Phospholipase A2—a mediator between proximal and distal effectors of inflammation, Immunol. Today 12 (5) (1991) 143–146, https://doi.org/10.1016/S0167-5699(05)80042-8.

[3] K.V. Ramana, S.K. Srivastava, Aldose reductase: a novel therapeutic target for inflammatory pathologies, Int. J. Biochem. Cell Biol. 42 (1) (2010) 17–20, https://doi.org/10.1016/j.biocel.2009.09.009.

[4] S.H. Choi, T. Sakamoto, O. Fukutomi, N. Inagaki, N. Matsuura, H. Nagai, A. Koda, Pharmacological study of phospholipase A2-induced histamine release from rat peritoneal mast cells, J. Pharmacobio-Dyn 12 (9) (1989) 517–522, https://doi.org/10.1159/000232607.

[5] L. Kaplan-Harris, J. Weiss, C. Mooney, S. Beckerdite-Quagliata, P. Elsbach, The action of human and rabbit serum phospholipase A2 on Escherichia coli phospholipids, JLR (J. Lipid Res.) 21 (5) (1980) 617–624, https://doi.org/10.1016/S0022-2275(20)42232-1.

[6] V.R. Kota, K.S. Satish, Aldose reductase: a novel therapeutic target for inflammatory pathologies, Int. J. Biochem. Cell Biol. 42 (1) (2010) 17–20, https://doi.org/10.1016/j.biocel.2009.09.009.

[7] U.C. Yadav, M. Shoeb, S.K. Srivastava, K.V. Ramana, Aldose reductase deficiency protects from autoimmune- and endotoxin-induced uveitis in mice, Investig. Ophthalmol. Vis. Sci. 52 (2011) 8076–8085, https://doi.org/10.1167/iovs.11-7830.

[8] U.C. Yadav, S.K. Srivastava, K.V. Ramana, Aldose reductase inhibition prevents endotoxin-induced uveitis in rats, Investig. Ophthalmol. Vis. Sci. 48 (2007) 4634–4642, https://doi.org/10.1167/iovs.07-0485.

[9] U.C. Yadav, M. Shoeb, S.K. Srivastava, K.V. Ramana, Aldose reductase deficiency protects from autoimmune- and endotoxin-induced uveitis in mice, Investig. Ophthalmol. Vis. Sci. 52 (2011) 8076–8085, https://doi.org/10.1167/iovs.11-7830.

[10] U.C. Yadav, K.V. Ramana, S.K. Srivastava, Aldose reductase inhibition suppresses airway inflammation, Chem. Biol. Interact. 191 (1) (2011) 339–345, https://doi.org/10.1016/j.cbi.2011.02.014.

[11] G.J. Zablocki, P.A. Ruzycki, M.A. Overturf, S. Palla, G.B. Reddy, J.M. Petrash, Aldose reductase-mediated induction of epithelium-to-mesenchymal transition (EMT) in lens, Chem. Biol. Interact. 191 (2011) 351–356, https://doi.org/10.1016/j.cbi.2011.02.005.

[12] R. Tammali, A.B. Reddy, K.V. Ramana, J.M. Petrash, S.K. Srivastava, Aldose reductase deficiency in mice prevents azoxymethane-induced colonic preneoplastic aberrant crypt foci formation, Carcinogenesis 30 (2009) 799–807, https://doi.org/10.1093/carcin/bgn246.

[13] R. Tammali, A.B. Reddy, A. Saxena, P.G. Rychahou, B.M. Evers, S. Qiu, S. Awasthi, K.V. Ramana, S.K. Srivastava, Inhibition of aldose reductase prevents colon cancer metastasis, Carcinogenesis 32 (2011) 1259–1267, https://doi.org/10.1093/carcin/bgr102.

[14] M. Del Poeta, W.A. Schell, C.C. Dykstra, S. Jones, R.R. Tidwell, A. Czarny, et al., Structure-in vitro activity relationships of pentamidine analogues and dication-substituted bis-benzimidazoles as new antifungal agents, Antimicrob. Agents Chemother. 42 (10) (1998) 2495–2502, https://doi.org/10.1128/aac.42.10.2495.

[15] R. Vinodkumar, S.D. Vaidya, B.V.S. Kumar, U.N. Bhise, S.B. Bhirud, U.C. Mashelkar, Synthesis, anti-bacterial, anti-asthmatic and anti-diabetic activities of novel N-substituted-2-(4-phenylethynyl-phenyl)-1H-benzimidazoles and N-substituted 2 [4-(4, 4-dimethyl-thiochroman-6-yl-ethynyl)-phenyl)-1H-benzimidazoles, Eur. J. Med. Chem. 43 (5) (2008) 986–995, https://doi.org/10.1016/j.ejmech.2007.06.013.

[16] J.R. Kumar, L. Jawahar, D. Pathak, Synthesis of benzimidazole derivatives: as anti-hypertensive agents, J. Chem. 3 (4) (2006) 278–285, https://doi.org/10.1155/2006/765712.

[17] G. Navarrete-Vázquez, R. Cedillo, A. Hernández-Campos, L. Yépez, F. Hernández-Luis, J. Valdez, et al., Synthesis and antiparasitic activity of 2-(trifluoromethyl) benzimidazole derivatives, Bioorg. Med. Chem. Lett 11 (2) (2001) 187–190, https://doi.org/10.1016/s0960-894x(00)00619-3.

[18] S. Graßmann, B. Sadek, X. Ligneau, S. Elz, C.R. Ganellin, J.-M. Arrang, et al., Progress in the proxifan class: heterocyclic congeners as novel potent and selective histamine H 3-receptor antagonists, Eur. J. Pharmaceut. Sci. 15 (4) (2002) 367–378, https://doi.org/10.1016/s0928-0987(02)00024-6.

[19] R. Sevak, A. Paul, S. Goswami, D. Santani, Gastroprotective effect of β 3 adrenoceptor agonists ZD 7114 and CGP 12177A in rats, Pharmacol. Res. 46 (4) (2002) 351–356, https://doi.org/10.1016/S1043-6618(02)00150-0.

[20] H. Göker, S. Özden, S. Yıldız, D.W. Boykin, Synthesis and potent antibacterial activity against MRSA of some novel 1, 2-disubstituted-1H-benzimidazole-N-alkylated-5-carboxamidines, Eur. J. Med. Chem. 40 (10) (2005) 1062–1069, https://doi.org/10.1016/j.ejmech.2005.05.002.
[21] D.O. Arnaiz, B. Griedel, S. Sakata, J.L. Dallas, M. Whitlow, L. Trinh, et al., Design, synthesis, and in vitro biological activity of benzimidazole based factor Xa inhibitors, Bioorg. Med. Chem. Lett 10 (9) (2000) 963–966, https://doi.org/10.1016/S0960-894X(00)00139-6.
[22] B. Can-Eke, M.O. Puskullu, E. Buyukbingol, M. Iscan, A study on the antioxidant capacities of some benzimidazoles in rat tissues, Chem. Biol. Interact. 113 (1) (1998) 65–77, https://doi.org/10.1016/s0009-2797(98)00020-9.
[23] L. Labanauskas, A. Brukštus, P. Gaidelis, V. Buchinskaite, E. Udrenaite, V. Daukšas, Synthesis and antiinflammatory activity of some new 1-acyl derivatives of 2-methylthio-5, 6-diethoxybenzimidazole, Pharmaceut. Chem. J. 34 (7) (2000) 353–355, https://doi.org/10.1023/A:1005213306544.
[24] N. Dege, M. Şekerci, S. Servi, M. Dinçer, Ü. Demirbas, Structure of 1-(thiophen-2-ylmethyl)-2-(thiophen-2-yl)-1H-benzimidazole, Turk. J. Chem. 30 (1) (2006) 103–108.
[25] M. Sabat, J.C. VanRens, M.J. Laufersweiler, T.A. Brugel, J. Maier, A. Golebiowski, M.J. Janusz, The development of 2-benzimidazole substituted pyrimidine based inhibitors of lymphocyte specific kinase (Lck), Bioorg. Med. Chem. Lett 16 (23) (2006) 5973–5977, https://doi.org/10.1016/j.bmcl.2006.08.132.
[26] Bhumika Agrahari, Samaresh Layek, Rakesh Ganguly, Necmi Dege, D. Devendra, Pathak,Synthesis, characterization and single crystal X-ray studies of pincer type Ni(II)-Schiff base complexes: application in synthesis of 2-substituted benzimidazoles, J. Organomet. Chem. 890 (2019) 13–20, https://doi.org/10.1016/j.jorganchem.2019.03.018. ISSN 0022-328X.
[27] N. Dege, M. Şekerci, S. Servi, M. Dinçer, U. Demirbaş, Structure of 1-(Thiophen-2-ylmethyl)-2-(thiophen-2-yl)-1H-benzimidazole, Article 12. Available at: Turk. J. Chem. 30 (1) (2006) https://journals.tubitak.gov.tr/chem/vol30/iss1/12.
[28] Mohd Muslim, Arif Ali, Musheer Ahmad, Abdullah Alarifi, Mohd Afzal, Nayim Sepay, Necmi Dege, A zinc(II) metal–organic complex based on 2-(2-aminophenyl)-1H-benzimidazole ligand: exhibiting high adsorption capacity for aromatic hazardous dyes and catecholase mimicking activity, J. Mol. Liq. 363 (2022) 119767, https://doi.org/10.1016/j.molliq.2022.119767. ISSN 0167-7322.
[29] M. Gaba, S. Singh, C. Mohan, Benzimidazole: an emerging scaffold for analgesic and anti-inflammatory agents, Eur. J. Med. Chem. 76 (2014) 494–505, https://doi.org/10.1016/j.ejmech.2014.01.030.
[30] K. Chkirate, K. Karrouchi, N. Dege, N. Kheira Sebbar, A. Ejjoummany, S. Radi, Y. Garcia, Co(ii) and Zn(ii) pyrazolyl-benzimidazole complexes with remarkable antibacterial activity, New J. Chem. (2020), https://doi.org/10.1039/c9nj05913j.
[31] R. Paramashivappa, P. Phani Kumar, P.V. Subba Rao, A. Srinivasa Rao, Design, synthesis and biological evaluation of benzimidazole/benzothiazole and benzoxazole derivatives as cyclooxygenase inhibitors, Bioorg. Med. Chem. Lett 13 (4) (2003) 657–660, https://doi.org/10.1016/s0960-894x(02)01006-5.
[32] Pinar Sen, Göknur Yasa Atmaca, Erdogmus Ali, Sibel Demir Kanmazalp, Necmi Dege, S. Zeki Yildiz, Peripherally tetra-benzimidazole units-substituted zinc(II) phthalocyanines: synthesis, characterization and investigation of photophysical and photochemical properties, J. Lumin. 194 (2018) 123–130, https://doi.org/10.1016/j.jlumin.2017.10.022. ISSN 0022-2313.
[33] G. Mariappan, R. Hazarika, F. Alam, R. Karki, U. Patangia, S. Nath, Synthesis and biological evaluation of 2-substituted benzimidazole derivatives, Arab. J. Chem. 8 (5) (2015) 715–719, https://doi.org/10.1016/j.arabjc.2011.11.008.
[34] S.L. Helfand, J. Werkmeister, J.C. Roder, Chemiluminescence response of human natural killer cells. I. The relationship between target cell binding, chemiluminescence, and cytolysis, J. Exp. Med. 156 (2) (1982) 492–505, https://doi.org/10.1084/jem.156.2.492.
[35] C.J. Morris, Carrageenan-induced paw edema in the rat and mouse, Inflammation protocols (2003) 115–121, https://doi.org/10.1385/1-59259-374-7:115.
[36] M. McGann, FRED pose prediction and virtual screening accuracy, J. Chem. Inf. Model. 51 (2011) 578–596, https://doi.org/10.1021/ci100436p.
[37] M. McGann, FRED and HYBRID docking performance on standardized datasets, J. Comput. Aided Mol. Des. 26 (8) (2012) 897–906, https://doi.org/10.1007/s10822-012-9584-8.
[38] T.W. Backman, Y. Cao, T. Girke, ChemMine tools: an online service for analyzing and clustering small molecules, Nucleic Acids Res. 39 (suppl_2) (2011) W486–W491, 10.1093/nar/gkr320.
[39] P.C. Hawkins, A.G. Skillman, G.L. Warren, B.A. Ellingson, M.T. Stahl, Conformer generation with OMEGA: algorithm and validation using high quality structures from the Protein Databank and Cambridge Structural Database, J. Chem. Inf. Model. 50 (4) (2010) 572–584, https://doi.org/10.1021/ci100031x.